AGU PUBLICATIONS

Geophysical Research Letters

RESEARCH LETTER
10.1002/2016GL068184

Key Points:
- The first multiparameter parameterizations of mixing efficiency and turbulent Prandtl number are proposed
- Global maps of mixing efficiency suggest local estimates that may be grossly different from the canonical value of 0.2
- Estimates of diapycnal diffusivity need to be reassessed based on the generalized-Osborn formula

Supporting Information:
- Supporting Information S1
- Figure S1
- Figure S2

Correspondence to:
H. Salehipour,
h.salehipour@utoronto.ca

Citation:
Salehipour, H., W. R. Peltier, C. B. Whalen, and J. A. MacKinnon (2016), A new characterization of the turbulent diapycnal diffusivities of mass and momentum in the ocean, *Geophys. Res. Lett.*, *43*, doi:10.1002/2016GL068184.

Received 9 FEB 2016
Accepted 9 MAR 2016
Accepted article online 12 MAR 2016

A new characterization of the turbulent diapycnal diffusivities of mass and momentum in the ocean

H. Salehipour[1], W. R. Peltier[1], C. B. Whalen[2], and J. A. MacKinnon[2]

[1]Department of Physics, University of Toronto, Toronto, Ontario, Canada, [2]Scripps Institution of Oceanography, University of California, San Diego, La Jolla, California, USA

Abstract The diapycnal diffusivity of mass supported by turbulent events in the ocean interior plays a fundamental role in controlling the global overturning circulation. The conventional representation of this diffusivity, due to Osborn (1980), assumes a constant mixing efficiency. We replace this methodology by a generalized-Osborn formula which involves a mixing efficiency that varies nonmonotonically with at least two nondimensional variables. Using these two variables, we propose dynamic parameterizations for mixing efficiency and turbulent Prandtl number (the latter quantifies the ratio of momentum to mass diapycnal diffusivities) based on the first synthesis of an extensive direct numerical simulation of inhomogeneously stratified shear-induced turbulence. Data from Argo floats are employed to demonstrate the extent of the spatial and statistical variability to be expected in both the diapycnal diffusivities of mass and momentum. We therefore suggest that previous estimates of these important characteristics of the global ocean require reconsideration.

1. Introduction

The return of abyssal waters to the ocean surface depends critically on the irreversible process of diapycnal mixing [*Munk*, 1966; *Talley*, 2013]. However, debate continues concerning the spatial and temporal variability of the efficiency of such mixing in the global oceans [*Peltier and Caulfield*, 2003; *Wunsch and Ferrari*, 2004; *Ivey et al.*, 2008]. An equally pressing issue that has not been sufficiently addressed, concerns the degree of momentum diffusion associated with the turbulent diapycnal diffusion of mass. In order to assess the possible spatial variability of these quantities, improved understanding of small-scale stratified turbulent mixing processes must be framed in a global context. Our goal in this paper is to take a significant step toward accomplishing this task by integrating the extensive direct numerical simulation (DNS) data set of *Salehipour and Peltier* [2015] (referred to hereinafter as [SP]) with the global strain measurements from Argo floats as reported in *Whalen et al.* [2012, 2015].

The conventional method for relating estimates of turbulent dissipation, ϵ, to turbulent diapycnal diffusivity, K_ρ, is based on a simplified turbulent kinetic energy (TKE) formula first proposed by *Osborn* [1980], namely:

$$K_\rho = \gamma \frac{\epsilon}{N^2} \tag{1}$$

in which $N^2 = -g/\rho_0(\mathrm{d}\overline{\rho}/\mathrm{d}z)$, where $\overline{\rho}$ denotes the mean flow density, and $\gamma = R_f/(1-R_f)$ is a "flux coefficient" based on the flux Richardson number, R_f (defined as the ratio of the buoyancy flux to the shear production of TKE), which is conventionally assumed to be a measure of mixing efficiency. Following the empirical suggestions of *Osborn* [1980] that $R_f \leq 0.17$, γ is frequently assumed to be fixed at $\gamma = 0.2$. We will hereinafter refer to this practice as the Osborn method. This formula suffers from two fundamental problems: (i) its underlying assumptions include homogeneous and statistically stationary flow conditions which are not strictly satisfied by actual oceanographic turbulent flows and (ii) the assumption of constant mixing efficiency is an oversimplification [*Smyth et al.*, 2001; *Ivey et al.*, 2008; *Mashayek and Peltier*, 2013].

The first problem has recently been resolved in SP in which the accurate representation of diapycnal diffusivity due to *Winters and D'Asaro* [1996] has been recast into an "Osborn-like" form (referred to hereinafter as the generalized-Osborn formula). Not only is this new formula valid for any Boussinesq flow (i.e., it relaxes the original limiting assumptions on which the Osborn formula is based) but also distinguishes between irreversible

and reversible processes while closely resembling the original Osborn formula. This generalized-Osborn formula has the following form (c.f. (1)):

$$K_\rho = \Gamma \frac{\epsilon}{N_*^2} \tag{2}$$

in which the flux coefficient $\Gamma = E/(1-E)$ depends on the precise definition of mixing efficiency, $E = \mathcal{M}/(\mathcal{M}+\epsilon)$ which invokes a time-dependent adiabatic restratification of the density field into a background stably stratified reference state whose buoyancy frequency is denoted by N_* and is associated with a state of minimum potential energy [*Winters et al.*, 1995; *Caulfield and Peltier*, 2000]. Through this "sorting" process, the buoyancy flux is essentially decomposed into a "reversible" (stirring) and an "irreversible" (mixing) component. Mixing, $\mathcal{M}$ (refer to SP for its explicit definition), therefore represents the rate at which available potential energy is dissipated irreversibly, whereas stirring is characterized by the reversible energy exchanges between the kinetic and potential energy reservoirs. This important distinction, which is neglected in the Osborn formula (1), is the basis on which the generalized-Osborn formula (2) is derived.

As to the second problem, the actual variability of mixing efficiency has remained enigmatic despite the consensus that it cannot be constant [*Ivey et al.*, 2008]. The current parameterizations of mixing efficiency (e.g., that of *Shih et al.* [2005]) are also highly contentious since all of them depend on a single parameter and are therefore inherently ambiguous [*Mater and Venayagamoorthy*, 2014]. Consequently, our aim is to propose the first multiparameter representation for E.

Besides the scalar diapycnal diffusivity, all numerical models that do not resolve subgrid scale turbulent processes also rely on a turbulence closure model that prescribes parameterizations for the momentum diffusivity (K_m) [e.g., *Klymak et al.*, 2010]. It is a common practice to use the turbulent Prandtl number for this purpose in order to relate the momentum and scalar diffusivities as $Pr_t = K_m/K_\rho$. To properly distinguish between reversible and irreversible contributions to the momentum flux, SP proposed a new formulation for K_m as

$$K_m = \frac{1}{1-E}\left(\frac{\epsilon}{S^2}\right) \tag{3}$$

in which $S = \mathrm{d}\bar{u}/\mathrm{d}z$ denotes the vertical shear of streamwise mean flow. Because (3) may be rewritten as $K_m = (Ri_*/E)K_\rho$, where $Ri_* = N_*^2/S^2$ is the gradient Richardson number based on the sorted density profile, a new formulation for Pr_t as $Pr_t = Ri_*/E$ is also implied which significantly extends the homogeneous formulations of *Venayagamoorthy and Stretch* [2010] to any Boussinesq flow and may be contrasted with its conventional definition as $Pr_t = Ri/R_f$ (see [SP] for further details).

A value of unity for Pr_t has commonly been assumed based on a physical argument that in a highly turbulent flow the turbulent diffusion rates of the momentum and scalar fields should be equal. For stably stratified flows, different empirical parameterizations have been proposed based on the gradient Richardson number that suggest Pr_t increases at higher Ri with $Pr_t \approx 1$ at low Ri [*Schumann and Gerz*, 1995; *Venayagamoorthy and Stretch*, 2010]. Again a key question of interest to us concerns the spatial variability of Pr_t throughout the world's oceans. In particular, we investigate whether the current assumption of a globally constant $Pr_t = 1$ (or even $Pr_t = 10$) [*Danabasoglu et al.*, 2012] is reasonable.

2. Methodology

2.1. Toward a Multiparameter Mixing Efficiency Parameterization

The multiparameter dependence of mixing efficiency in stratified shear flows suggests that E must be prescribed in at least a three-dimensional parameter space, for example, as a function of the molecular Prandtl number ($Pr = \nu/\kappa$, where ν is the kinematic viscosity and κ is the molecular diffusivity), the gradient Richardson number ($Ri = N^2/S^2$) and the buoyancy Reynolds number ($Re_b = \epsilon/(\nu N^2)$). Recent investigations of the stratified turbulence generated by breaking nonlinear Kelvin-Helmholtz (KH) waves at sufficiently high Reynolds numbers explicitly demonstrate such a dependence on Ri [*Mashayek et al.*, 2013; SP], Pr [*Salehipour et al.*, 2015], and Re_b [SP]. While it is certain that E depends on Pr [*Smyth et al.*, 2001; *Salehipour et al.*, 2015], we assume for present purposes that the dependences on Re_b and Ri are dominant. This assumption reduces the representation of E to a two-dimensional parameter space expressed as $E = f(Ri, Re_b)$.

In order to infer $E = f(Ri, Re_b)$, we employ the DNS data set of SP as well as two additional DNS analyses of the same problem but with extremely high values of the initial Reynolds number at $Re = 2 \times 10^4$ and $Re = 3 \times 10^4$ (see the supporting information for further details). Furthermore, we split the parameter space

into a region where E rises with Re_b (left flank) and a region in which E decreases with Re_b (right flank), respectively, associated with the buoyancy-dominated and shear-dominated regimes [SP]. We denote the peak value of E at which the rollover occurs and its corresponding Re_b as $E^\star$ and $Re_b^\star$, respectively.

Our DNS-constrained representation of $E(Ri, Re_b)$ may then be written as

$$\frac{E}{E^\star} = \frac{(1+2p)\left(\frac{Re_b}{Re_b^\star}\right)^p}{1+2p\left(\frac{Re_b}{Re_b^\star}\right)^{p+0.5}} \tag{4}$$

in which $p = 0.55$ if $Re_b \le Re_b^\star$ and $p = 1$ if $Re_b > Re_b^\star$ representing the left and right "flanks" respectively. The Ri dependence is embedded explicitly in $E^\star$ and $Re_b^\star$, defined respectively as follows:

$$E^\star(Ri) = \frac{3\left(\frac{Ri}{Ri^\star}\right)}{8+\left(\frac{Ri}{Ri^\star}\right)^9}, \tag{5}$$

$$Re_b^\star(Ri) = \frac{4}{9}\left(\frac{\Psi}{E^\star}\right)^2, \tag{6}$$

$$\Psi(Ri) = 0.04\exp(12Ri) + 1.5, \tag{7}$$

where $Ri^\star = 0.4$ in (5) denotes the Ri value associated with the peak value of $E^\star$ in its nonmonotonic variation with Ri. Furthermore, $Re_b^\star(Ri)$ in (6) essentially employs a supplementary variable, Ψ (7), that is obtained by setting $E \sim \Psi Re_b^{-0.5}$ in the limit of $Re_b/Re_b^\star \to \infty$.

Note that in this paper, both the N and S profiles are first squared and then vertically averaged over the depth of the turbulent patch. The resulting values of Ri inferred from our DNS database hence lie in the range $0 < Ri < 0.5$ which partly covers the observed values of Ri in the ocean [see, e.g., *Polzin*, 1996; *Smyth and Moum*, 2013; *van Haren et al.*, 2014]. For the purpose of this paper, we have assumed $E \to 0$ as $Ri \to 1$.

Figure 1a illustrates the distribution of E in the $Ri - Re_b$ space as parameterized by (4). The Ri variation of $Re_b^\star$ as per (6) is also shown in this figure by a dashed curve. Furthermore, Figure 1c plots $E^\star(Ri)$ and $\Psi(Ri)$ as obtained from the DNS data together with the inferred nonlinear least squares fits of (5) and (7). The supporting information describes the procedure that was employed to construct the components of this parameterization.

Although it is well established that E varies nonmonotonically with Ri [*Linden*, 1979; *Strang and Fernando*, 2001; *Mashayek et al.*, 2013; SP], the nonmonotonic dependence of E on Re_b [*Barry et al.*, 2001; *Shih et al.*, 2005; SP] has been actively disputed (see, e.g., *Gregg et al.* [2012] and *Bouffard and Boegman* [2013] for a discussion). This dual nonmonotonicity has been nonetheless explicitly realized in the DNS analyses of SP and is therefore preserved in the proposed parameterization through the continuous transition between the left and right flanks at $Re_b^\star$ and the nonmonotonic dependence of $E^\star$ on Ri.

On the "right flank" the $Re_b^{-0.5}$ power law relation, implicit in (4) with $p = 1$ when $Re_b \gg Re_b^\star$, has been adopted here because of the accumulating DNS [*Shih et al.*, 2005; SP] and observational [*Davis and Monismith*, 2011; *Lozovatsky and Fernando*, 2013; *Bouffard and Boegman*, 2013; *Bluteau et al.*, 2013; *Walter et al.*, 2014; *Monismith et al.*, 2015] evidence that mixing efficiency does decrease with Re_b as $E = \Psi Re_b^{-0.5}$. For example, *Monismith et al.* [2015] reported $\Psi \sim 1.5 - 4.5$ for a series of observations with $10^2 < Re_b < 10^7$. Our DNS data suggest that Ψ may indeed increase exponentially with Ri as in (7) and may lie in the range $1 < \Psi < 15$ for $0 < Ri < 0.5$. The high Ri regions of the parameter space are yet to be explored by DNS of "strongly" stratified turbulence and thus should be interpreted as preliminary. This uncertainty is indicated in Figure 1c by a shaded area.

A number of interesting observations follow from Figure 1a: (i) irreversible mixing becomes as efficient as $E \sim 1/3$ (or $\Gamma \sim 0.5$) for relatively high levels of stratification with $Ri \sim 0.35 - 0.45$ which occurs in the range $\mathcal{O}(10^2) < Re_b < \mathcal{O}(10^3)$. (ii) This highly efficient mixing is sustained for a broader range of Re_b if the flow is

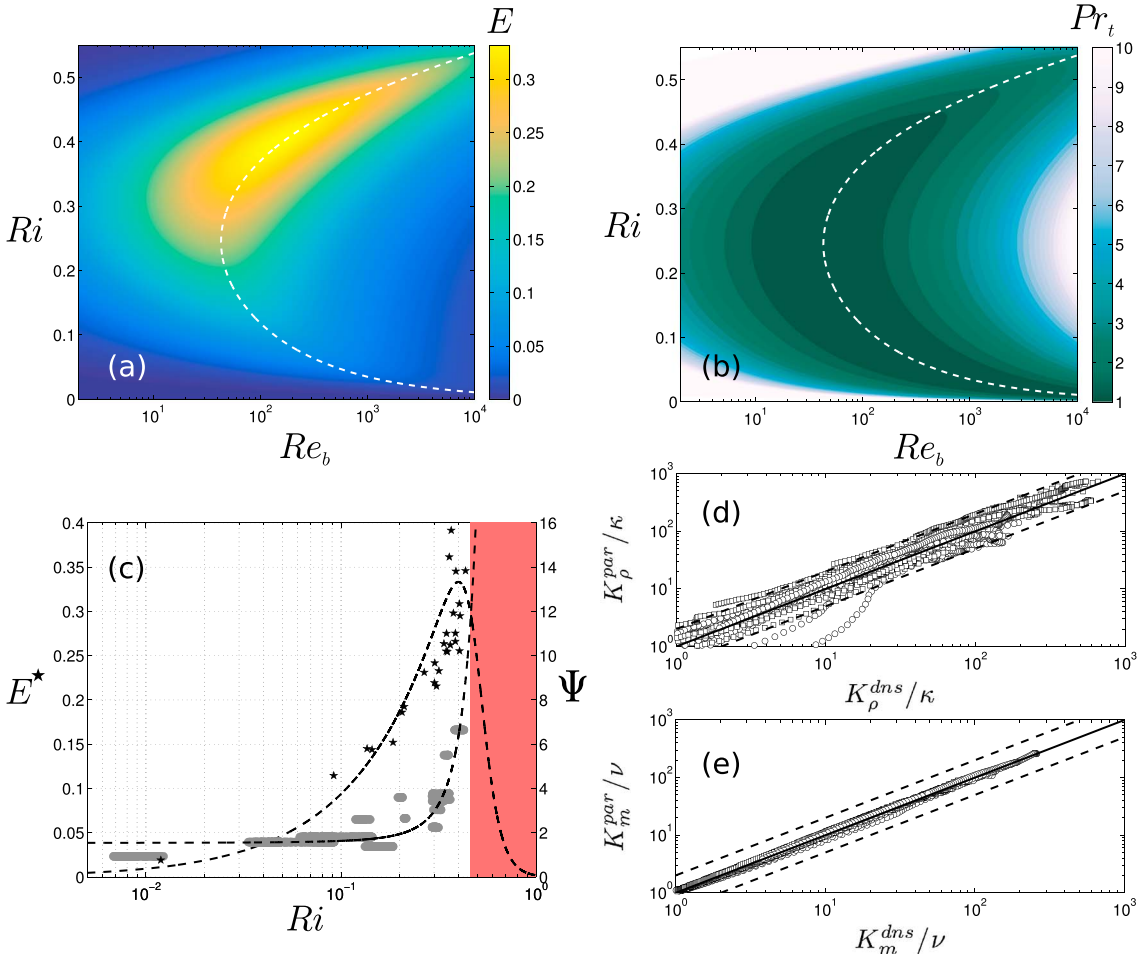

Figure 1. Contours of (a) $E = f(Re_b, Ri)$ as parameterized in (4) (to be compared with the fixed canonical value of $R_f = 0.17$ in the Osborn formula) and (b) $Pr_t = Ri_*/E$. The dashed curves in Figures 1a and 1b illustrate $Re_b^\star$ (6). (c) Illustration of $\Psi(Ri)$ (7) (gray circles) and $E^\star(Ri)$ (5) (black stars) as inferred from DNS analyses. The shaded area in Figure 1c corresponds with the uncertain region of high-*Ri*. (d, e) Comparison between the parameterized K_ρ and K_m (denoted by K_ρ^{par} and K_m^{par}) with their DNS-based origins (denoted by K_ρ^{dns} and K_m^{dns}) at $Pr = 1$ (circles) and $Pr > 1$ (squares). The dashed lines identify a factor of 2 underestimation/overestimation.

sufficiently stratified. (iii) $Re_b^\star(Ri)$ varies nonmonotonically with a minimum of $Re_b^\star \sim 40$ at $Ri = 0.25$ which increases for higher and lower values of *Ri* (note that due to the smooth form of *E* around $Re_b^\star$, *E* becomes $\propto Re_b^{-0.5}$ at $\sim 9/4 Re_b^\star$, e.g., at $Re_b \sim 90$ for $Ri = 0.25$). The increase in $Re_b^\star$ at higher *Ri* occurs because, as the flow becomes more strongly stratified, the transition to the shear-dominated turbulent regime (i.e., right flank) requires increasingly more energetic turbulence and thus $Re_b^\star$ ought to increase. On the other hand, $Re_b^\star$ also has to increase dramatically as $Ri \to 0$ since, in order for the resulting buoyancy-dominated turbulence to become shear-dominated, significant turbulent dissipation is required. (iv) The transition to the right flank in *Shih et al.* [2005] at $Re_b \sim 100$, as also reinforced by SP, occurs because in both studies high Re_b was only obtained due to relatively weak stratification. In fact, our exceptionally expensive DNS analyses with initial Reynolds numbers up to 3×10^4 have revealed that high Re_b on the right flank may also be achieved at high *Ri* if the Reynolds number is sufficiently high.

To assess the parameterized values of *E* against the original DNS-based values, Figure 1d employs the generalized-Osborn formula in (2) to compare the resulting values of K_ρ/κ. As shown in this figure, the DNS data at $Pr = 1$ are represented quite accurately, while those at higher *Pr* are mostly overestimated by the parametrization but are still within a factor of 2. This overestimation is partly because the *Pr* effect has been neglected in this preliminary form of the parameterization. Furthermore, the accuracy of the proposed parameterization will be realized by comparing K_ρ^{dns} against traditional models of *Osborn* [1980] and *Osborn and Cox* [1972] as has been done explicitly in Figure 2 of SP.

2.2. Toward a Multiparameter Pr_t Parameterization

The proposed multiparameter representation of E in (4) directly implies a multiparameter representation of $Pr_t = g(Ri, Re_b)$ after recalling that $Pr_t = Ri_*/E$ and $Ri_* \sim Ri$ (or $N \sim N_*$) due to vertical averaging [SP]. We will hereinafter use Ri and Ri_* interchangeably. Notice that in the absence of diapycnal diffusivity (i.e., $K_\rho = 0$), K_m will maintain nonzero values because internal waves would still sustain momentum flux across isopycnals. Therefore, if $K_\rho = 0$, Pr_t loses its utility and K_m is best described as $K_m = \epsilon/S^2$ (see (3) for $E = 0$).

Figure 1b illustrates such dual dependence in the $Ri - Re_b$ space (the dashed curve again indicates $Re_b^\star$ (6) and thus distinguishes the left and right flanks). As shown in this figure, Pr_t increases with Ri from ~ 1 at relatively low Ri values in accord with the previous Ri-based parametrizations. However, in contrast to all previously suggested parameterizations, the dependence on Ri critically depends also upon Re_b. For example, at high Re_b where turbulence is highly energetic, Pr_t varies nonmonotonically with Ri and rises to values as high as $Pr_t \sim \mathcal{O}(10)$ for moderate values of Ri. This counter-intuitive rise of Pr_t is due to the right flank decrease of E with Re_b at moderate Ri and clearly is not in accord with the common assumption of $Pr_t \sim 1$ for intensely turbulent patches. Finally, in a particular region of the $Ri - Re_b$ space (and not necessarily at low Ri) momentum and mass turbulent diffusivities tend to be equal resulting in $Pr_t \sim 1$. It is very interesting to note that, this region of the parameter space coincides with that in which mixing is most efficient.

Similar to Figure 1d, Figure 1e evaluates the parameterized momentum diffusivity K_m/ν against that obtained directly from the DNS data set based on (3). The excellent agreement should not be surprising (as also noted by SP) because unlike K_ρ, K_m is almost insensitive to E unless $E \to 1$ (c.f. (2) and (3)).

2.3. Application to the Global Oceans

In order to apply the DNS-constrained parameterizations to the global ocean, we will rely on two major assumptions:

1. The mixing properties of the idealized KH-ansatz are statistically representative of individual oceanic mixing events.
2. The *average* diapycnal mixing supported by a fine-scale internal wavefield is similar to that induced by a turbulent patch, *provided that* their corresponding averaged values of Re_b and Ri are similar.

While the first notion was suggested by *Smyth et al.* [2001], the second assumption follows from the universality conjecture of SP. The latter is based on the striking similarity observed between the DNS results of the KH-ansatz and those of a homogeneously sheared and stratified flow [*Shih et al.*, 2005], despite their different forcing mechanism and spatial and temporal scales.

Under these assumptions and according to the earlier discussions, global maps of E (or Γ) and Pr_t require a priori knowledge of the global distribution of both Ri and Re_b. While microstructure measurements may provide the needed information, their global distribution does not provide adequate spatial coverage [*Waterhouse et al.*, 2014]. Alternatively, the global array of Argo float profiles provides a suitable means of inferring the global distribution of Re_b by invoking the fine-scale parameterization approach to estimate turbulent dissipation [*Polzin et al.*, 2014] but lacks the measurements of the mean flow shear and hence Ri (see the supporting information for details).

While the assumptions underlying the fine-scale parameterization imply that it is inappropriate for some environments, it agrees in an unbiased manner with microstructure measurements within a factor of 2–3 in a variety of open ocean conditions including one region close to the equator [*Whalen et al.*, 2015]. Thus, the fine-scale parameterization is assumed to be appropriate for inferring the global-scale patterns in the following discussion despite its essential caveats as documented in *Whalen et al.* [2015].

3. Results

Global maps showing the 8 year mean values of the inferred $Re_b = \epsilon/(\nu N^2)$ (assuming $\nu = 10^{-6}$ m^2/s) as well as the parameterized estimates of the flux coefficient $\Gamma = E/(1-E)$ (see (4)), and the turbulent Prandtl number, $Pr_t = Ri_*/E$ are presented in Figure 2 for a depth interval of 250–450 m. The results of our analysis at all depth levels are consolidated in Figure 3 in terms of histograms of Re_b, Γ, K_ρ, and K_m, where the latter two have been computed using (2) and (3). The available depth-dependent inferred dissipation rates are associated with segments centered in 200 m bins covering the depth of 250–2000 m and are averaged into 1.5° square bins using data from *Whalen et al.* [2015]. Notice that globally constant values of either $Ri = 0.25$ (a commonly

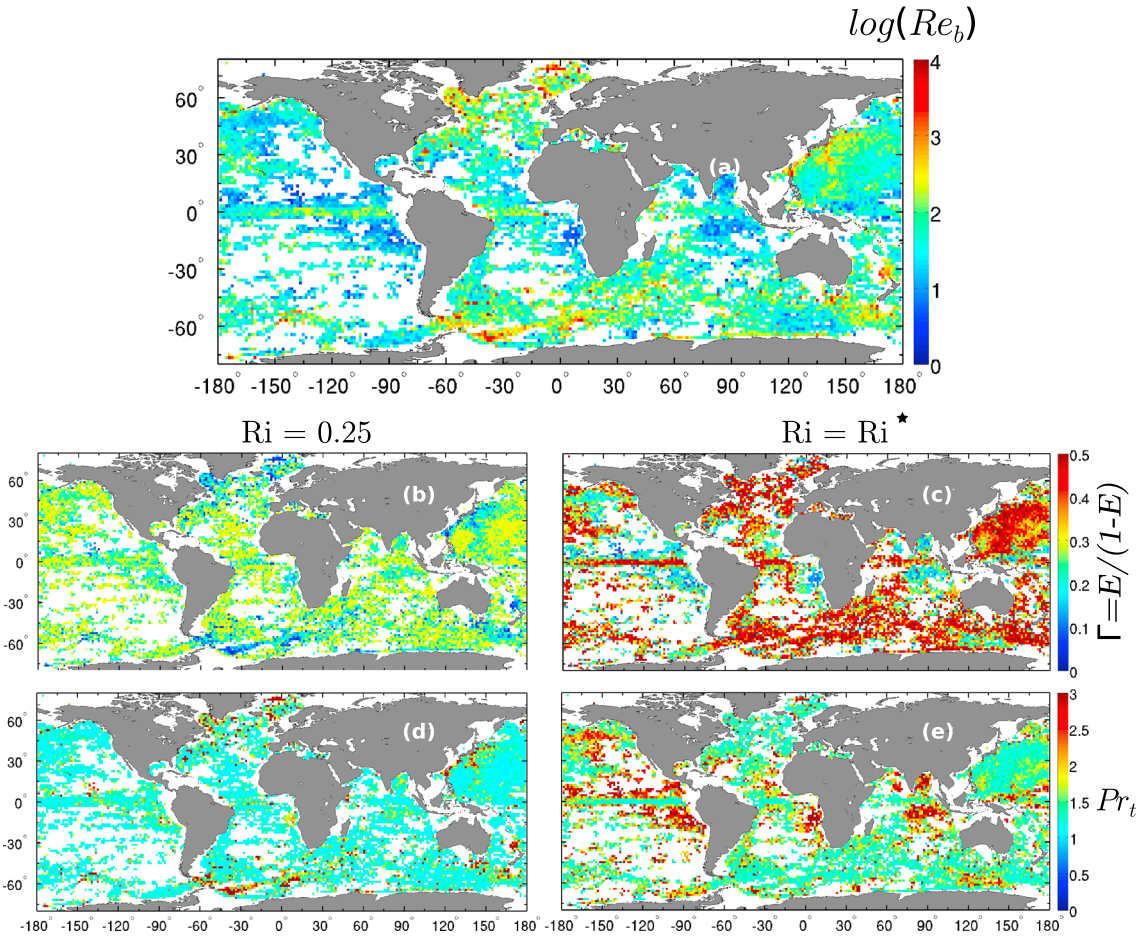

Figure 2. (a) $Re_b = \epsilon/(\nu N^2)$ in which ϵ and N^2 are inferred from over 8 years (2006–2014) of Argo data. Estimates from high-vertical resolution data centered between 250 and 450 m are averaged over 1.5° square bins and plotted if they contain more than three dissipation rate estimates [*Whalen et al.*, 2012, 2015]. (b, c) Parameterized global estimates of $\Gamma = E/(1-E)$, as per (4) using the Re_b map in Figure 2a and assuming $Ri = 0.25$ or $Ri = Ri^\star$. (d, e) Parameterized global estimates of $Pr_t = Ri_*/E$, using the Re_b map in Figure 2a and assuming $Ri = 0.25$ or $Ri = Ri^\star$.

observed value associated with marginal instability, see *Smyth and Moum* [2013]) or $Ri = Ri^\star \sim 0.35 - 0.45$ are assumed in Figure 2. For illustrative purposes, Figure 3 also assumes $Ri = 0.1 < 0.25$ in addition to the previous two Ri values. As noted earlier, $Ri^\star$ corresponds to the highest $E^\star$ point in the parameter space of Figure 1a. The precise value of $Ri^\star$ depends on parameterization details and will not affect our discussion to follow.

The results in Figures 2a and 3a demonstrate that Re_b varies over 4 orders of magnitude, ranging between $\mathcal{O}(10^0)$ and $\mathcal{O}(10^4)$. The horizontally averaged value of Re_b lies in the range $90 - 180$ for all depth levels. Commensurate variations of E and Pr_t are therefore expected based on the mixing properties of small-scale shear-driven stratified turbulence. In particular as shown in Figures 2b, 2c, and 3b, for $Ri = 0.25$ (or $Ri = Ri^\star$), the value of $\Gamma = E/(1-E)$ varies in the range $0 \leq \Gamma \leq 0.25$ (or $0 \leq \Gamma \leq 0.5$ for $Ri = Ri^\star$) throughout the ocean with a global mean of $\Gamma \sim 0.25$ (or $\Gamma \sim 0.3$ for $Ri = Ri^\star$). These estimates may be reduced by a factor of 1.2–1.5 if the role of Pr is considered [see *Salehipour et al.*, 2015, Figure 14d].

Depending on Ri, there may also exist prominent variability in regions with either high or low Re_b. For example, Figure 2b at $Ri = 0.25$ would suggest that in the Southern Ocean Γ is significantly less than the global mean value of ~ 0.2 in the Drake Passage, as well as over the Southwest Indian and Macquarie Ridges. This reduced mixing efficiency is due to the intensified turbulence leading to high values of Re_b in these regions which are characterized by rough bottom topography. The pattern of energetic turbulence and hence reduced mixing efficiency over regions of rough topography in the Southern Ocean seems to persist throughout the entire top 2 km of the ocean assuming that $Ri = 0.25$. North of New Zealand, mixing also seems to be relatively

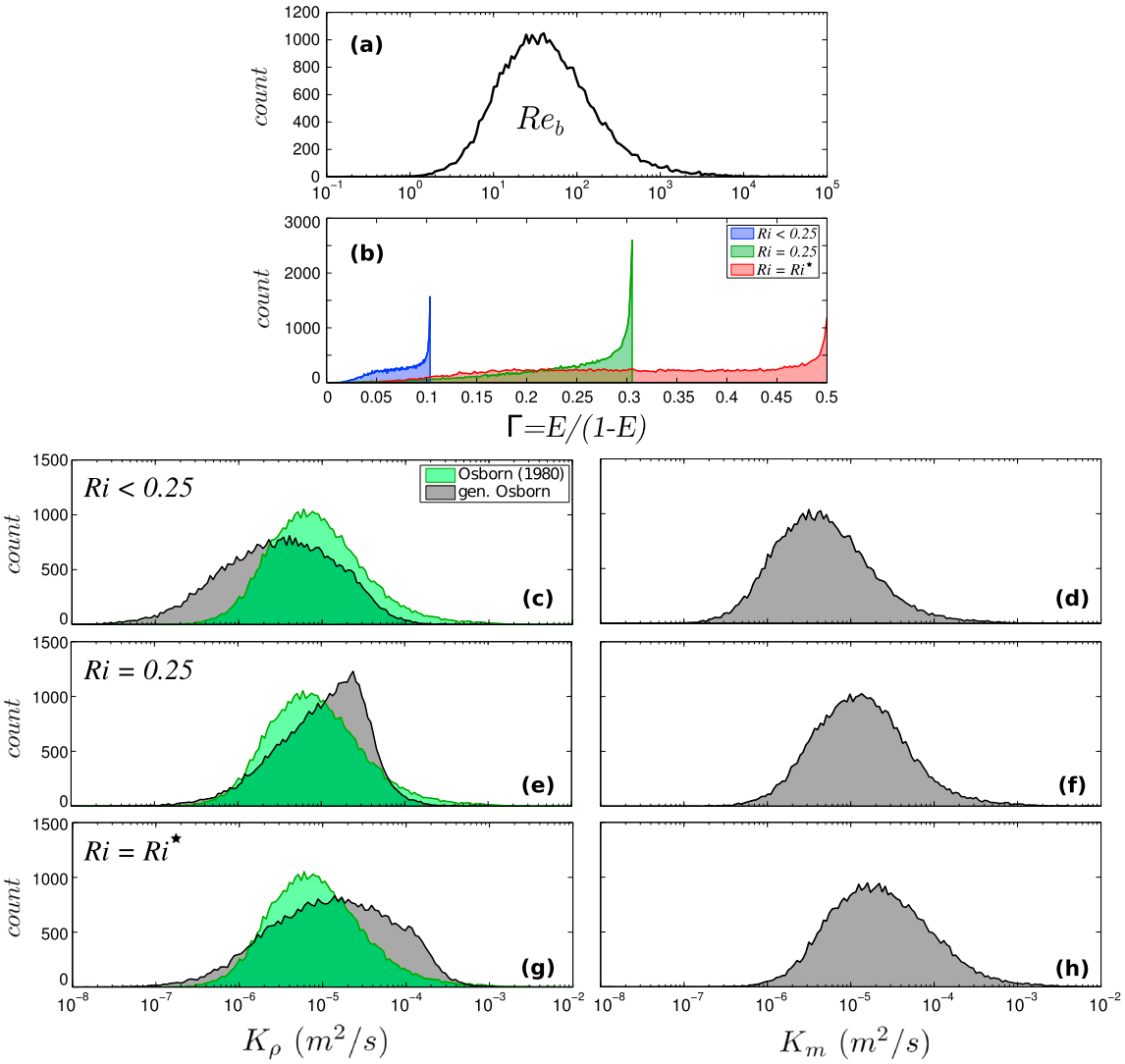

Figure 3. Histograms of (a) $Re_b = \epsilon/(\nu N^2)$ and (b) $\Gamma = E/(1-E)$ based on the new parameterization with constant values of *Ri*; (c, e, and g) K_ρ based on the Osborn and generalized-Osborn formulae; (d, f, and h) K_m as per (3). Argo data at all depth levels are employed in constructing these histograms.

inefficient due to high estimates of Re_b. In contrast, examples of much lower estimates of mixing efficiency that are due to extremely low values of Re_b include the Bay of Bengal, the Peru Basin, and the Angola Plain.

Figures 2d and 2e also depict the global distribution of the parameterized Pr_t for the same two *Ri* values. Our results do not support the use of $Pr_t = 10$ [*Large et al.*, 1994; *Danabasoglu et al.*, 2012] unless the ocean is assumed to be quiescent (i.e., $Re_b = \mathcal{O}(10^0)$) or extremely energetic (i.e., $Re_b \gtrsim \mathcal{O}(10^4)$). For $Ri = 0.25$, Pr_t reaches 3 sporadically (e.g., in the Drake Passage) but it is generally lower in all depth levels. The globally averaged estimates of our parameterized Pr_t are much closer to $Pr_t \approx 1-2$ for the top 2 km of the ocean. These global estimates may *increase* by a factor of 1.2–1.5 if the role of *Pr* is considered. The sensitivity of ocean general circulation models (OGCMs) to such changes in Pr_t remains unknown.

The histograms in Figures 3c–3h demonstrate the direct implications of the proposed parameterizations upon the characterization of K_ρ and K_m. As expected, K_m is insensitive to the variability of *E* (because $E \nrightarrow 1$) but changes with *Ri* as $K_m/\nu = RiRe_b/(1-E)$ (see (3)). On the other hand, the distribution of K_ρ is highly sensitive to *E* and differs substantially with that estimated by the Osborn method based on the canonical spatially invariant fixed value of $\gamma = 0.2$ (see (1)).

If all small-scale mixing events were assumed to be optimally efficient (i.e., $Ri \sim Ri^\star$, see Figure 3g), mixing would typically occur more efficiently than is represented by $\gamma = 0.2$, causing a larger K_ρ than is predicated

by the Osborn formulation. On the other hand, if $Ri \ll Ri^\star$ or $Ri \gg Ri^\star$ (e.g., see Figure 3c), the flux coefficient and therefore K_ρ would be smaller than the values that are produced using the Osborn formulation (e.g., in the Southern Ocean and in the vicinity of the Drake passage).

The Diapycnal and Isopycnal Mixing Experiment in the Southern Ocean have focused on turbulent mixing through both microstructure measurements [*St. Laurent et al.*, 2012] and tracer release experiments [*Ledwell et al.*, 2011; *Watson et al.*, 2013]. The former method employs the Osborn formula with $\gamma = 0.2$. The average estimates of K_ρ inferred from these two methods differ slightly. While the difference between the measurement seasonality has been suggested to be an underlying reason for this discrepancy, the essential dependence of K_ρ on a variable mixing efficiency, as suggested by the histograms in Figure 3, may provide another, perhaps complementary, explanation.

4. Conclusion

Based on our improved understanding of small-scale shear-induced stratified turbulence produced through Kelvin-Helmholtz instability (i.e., the KH-ansatz), we have demonstrated in this letter the variability of mixing efficiency (E) and turbulent Prandtl number (Pr_t) that arises because of their dependence upon both the buoyancy Reynolds number, $Re_b = \epsilon/(\nu N^2)$, as well as the gradient Richardson number, $Ri = N^2/S^2$. New multiparameter parameterizations for both E and Pr_t have been introduced which directly imply that K_ρ and $K_m = Pr_t K_\rho$ should incorporate the influence of not only spatially varying turbulent dissipation (ϵ) and density stratification (N^2) but also a spatially varying E and Pr_t.

By inferring Re_b from Argo float data and by assuming globally constant Ri values, we have shown that the resulting global maps of $\Gamma = E/(1-E)$ (i) depend critically on Ri and (ii) may involve significant spatial variability which contrasts substantially with the assumption of a canonical flux coefficient of 0.2. Furthermore, the nonmonotonic dependence of E on Re_b at moderate levels of stratification implies that $K_m \gg K_\rho$, in contrast to the common assumption that $Pr_t = 1$ for highly turbulent flows. Nevertheless, such high Pr_t values are only sporadically observed in the top 2 km of the ocean which is why on average $Pr_t \approx 1 - 2$.

These interesting findings should be further examined for deep and abyssal waters where the diapycnal mixing structure is understood to be strongly controlled by dissipation of the internal tide forced either by the flow of the barotropic tide [*Garrett and Kunze*, 2007; *Klymak et al.*, 2012] or geostrophic eddies [*Nikurashin and Ferrari*, 2011; *Nikurashin et al.*, 2013] over ocean bottom topography.

The currently prevalent view regarding the magnitude and depth-dependent trend of K_ρ [see, e.g., *Waterhouse et al.*, 2014] is entirely based on the conventional approach of utilizing the Osborn formula with a flux coefficient of 0.2. Our revised parameterization for mixing efficiency embodied in the generalized-Osborn formula suggests that reconsideration of this view is warranted.

Previous studies have shown significant sensitivity of large-scale climate models to the horizontal and vertical distribution of K_ρ [*Jochum*, 2009; *Jayne*, 2009; *Saenko et al.*, 2012; *Melet et al.*, 2013]. For example, in the context of paleoclimate modeling, *Peltier and Vettoretti* [2014] and *Vettoretti and Peltier* [2015] have demonstrated that the intensely nonlinear Dansgaard-Oeschger oscillation, that is characteristic of cold glacial climate conditions, is highly sensitive to the representation of K_ρ. This letter provides the physical rationale for constraining the variability of E and subsequently for developing a revised representation of K_ρ to be employed in future sensitivity studies of both the modern and the glacial ocean.

Although the proposed parameterizations significantly extend the previous single-parameter representations (e.g., that of *Shih et al.* [2005] for E) to a multiparameter framework as previously suggested to be necessary by *Mater and Venayagamoorthy* [2014], they should be regarded as a preliminary attempt to connect the idealized studies of individual stratified mixing events to our understanding of global ocean mixing. Furthermore, the new characterizations may require further refinement prior to their implementation in an OGCM in order to relate the coarsely resolved OGCM estimates of Ri to those associated with small-scale turbulence as defined and employed in this letter.

Future efforts will be required (i) to understand the mixing properties of stratified turbulent flows induced by processes other than mean flow shear: e.g., by double-diffusion; (ii) to investigate whether there might be a "universal" characteristic behavior associated with stratified turbulent mixing as, e.g., conjectured by SP; (iii) to study the existence and strength of turbulent mixing in *strongly* stratified flows with $Ri > 0.5$; and

(iv) to understand the role of molecular Prandtl number (*Pr*) on high-Re_b shear-dominated flows. This will enable future adjustments to this parameterization in order to better represent the thermal, saline, and mixed stratification regimes observed in the ocean.

Acknowledgments
The authors appreciate the constructive comments of the three anonymous reviewers which have led to substantial improvements of the paper. This work has also benefited from interactions of H.S. and W.R.P. with A. Mashayek and C.P. Caulfield. The research of W.R.P. in Toronto is funded by NSERC Discovery grant A9627. All data employed for the analyses reported in this paper are properly cited and referred to in the reference list and in the supporting information file.

References

Barry, M. E., G. N. Ivey, K. B. Winters, and J. Imberger (2001), Measurements of diapycnal diffusivities in stratified fluids, *J. Fluid Mech.*, *442*, 267–291.
Bluteau, C. E., N. L. Jones, and G. N. Ivey (2013), Turbulent mixing efficiency at an energetic ocean site, *J. Geophys. Res. Oceans*, *118*(9), 4662–4672.
Bouffard, D., and L. Boegman (2013), A diapycnal diffusivity model for stratified environmental flows, *Dyn. Atmos. Oceans*, *61*, 14–34.
Caulfield, C. P., and W. R. Peltier (2000), The anatomy of the mixing transition in homogeneous and stratified free shear layers, *J. Fluid Mech.*, *413*, 1–47.
Danabasoglu, G., S. C. Bates, B. P. Briegleb, S. R. Jayne, M. Jochum, W. G. Large, S. Peacock, and S. G. Yeager (2012), The CCSM4 ocean component, *J. Clim.*, *25*(5), 1361–1389.
Davis, K., and S. Monismith (2011), The modification of bottom boundary layer turbulence and mixing by internal waves shoaling on a barrier reef, *J. Phys. Oceanogr.*, *41*(11), 2223–2241.
Garrett, C., and E. Kunze (2007), Internal tide generation in the deep ocean, *Annu. Rev. Fluid Mech*, *39*, 57–87.
Gregg, M., M. Alford, H. Kontoyiannis, V. Zervakis, and D. Winkel (2012), Mixing over the steep side of the Cycladic Plateau in the Aegean sea, *J. Marine Syst.*, *89*(1), 30–47.
Ivey, G. N., K. B. Winters, and J. R. Koseff (2008), Density stratification, turbulence, but how much mixing?, *Annu. Rev. Fluid Mech.*, *40*, 169–184.
Jayne, S. R. (2009), The impact of abyssal mixing parameterizations in an ocean general circulation model, *J. Phys. Oceanogr.*, *39*(7), 1756–1775.
Jochum, M. (2009), Impact of latitudinal variations in vertical diffusivity on climate simulations, *J. Geophys. Res.*, *114*, C01010.
Klymak, J. M., S. Legg, and R. Pinkel (2010), A simple parameterization of turbulent tidal mixing near supercritical topography, *J. Phys. Oceanogr.*, *40*(9), 2059–2074.
Klymak, J. M., S. Legg, M. H. Alford, M. Buijsman, R. Pinkel, and J. D. Nash (2012), The direct breaking of internal waves at steep topography, *Oceanography*, *25*(2), 150–159.
Large, W. G., J. C. McWilliams, and S. C. Doney (1994), Oceanic vertical mixing: A review and a model with a nonlocal boundary layer parameterization, *Rev. Geophys.*, *32*(4), 363–403.
Ledwell, J. R., L. C. St. Laurent, J. B. Girton, and J. M. Toole (2011), Diapycnal mixing in the Antarctic circumpolar current, *J. Phys. Oceanogr.*, *41*(1), 241–246.
Linden, P. F. (1979), Mixing in stratified fluids, *Geophys. Astrophys. Fluid Dyn.*, *13*, 3–23.
Lozovatsky, I. D., and H. J. S. Fernando (2013), Mixing efficiency in natural flows, *Phil. Trans. R. Soc. A*, *371*, 1–9.
Mashayek, A., and W. R. Peltier (2013), Shear induced mixing in geophysical flows: Does the route to turbulence matter to its efficiency?, *J. Fluid Mech.*, *725*, 216–261.
Mashayek, A., C. P. Caulfield, and W. R. Peltier (2013), Time-dependent, non-monotonic mixing in stratified turbulent shear flows: Implications for oceanographic estimates of buoyancy flux, *J. Fluid Mech.*, *736*, 570–593.
Mater, B. D., and S. K. Venayagamoorthy (2014), The quest for an unambiguous parameterization of mixing efficiency in stably stratified geophysical flows, *Geophys. Res. Lett*, *41*(13), 4646–4653.
Melet, A., R. Hallberg, S. Legg, and K. Polzin (2013), Sensitivity of the ocean state to the vertical distribution of internal-tide-driven mixing, *J. Phys. Oceanogr.*, *43*(3), 602–615.
Monismith, S., M. Squibb, R. Walter, C. Woodson, J. Dunkley, G. Pawlak, and J. Koseff (2015), *Direct Measurements of Turbulent Buoyancy Fluxes in the Nearshore Coastal Ocean*, Euromech Colloquium, Cambridge, U. K.
Munk, W. H. (1966), Abyssal recipes, *Deep-Sea Res.*, *113*, 207–230.
Nikurashin, M., and R. Ferrari (2011), Global energy conversion rate from geostrophic flows into internal lee waves in the deep ocean, *Geophys. Res. Lett.*, *38*(8), L08610.
Nikurashin, M., G. K. Vallis, and A. Adcroft (2013), Routes to energy dissipation for geostrophic flows in the Southern Ocean, *Nat. Geosci.*, *6*(1), 48–51.
Osborn, T. R. (1980), Estimates of the local rate of vertical diffusion from dissipation measurements, *J. Phys. Oceanogr.*, *10*, 83–89.
Osborn, T. R., and C. S. Cox (1972), Oceanic fine structure, *Geophys. Astrophys. Fluid Dyn.*, *3*(1), 321–345.
Peltier, W. R., and C. P. Caulfield (2003), Mixing efficiency in stratified shear flows, *Annu. Rev. Fluid Mech.*, *35*, 135–167.
Peltier, W. R., and G. Vettoretti (2014), Dansgaard-Oeschger oscillations predicted in a comprehensive model of glacial climate: A "kicked" salt oscillator in the atlantic, *Geophys. Res. Lett.*, *41*(20), 7306–7313.
Polzin, K. (1996), Statistics of the Richardson number: Mixing models and finestructure, *J. Phys. Oceanogr.*, *26*(8), 1409–1425.
Polzin, K. L., A. C. Naveira Garabato, T. N. Huussen, B. M. Sloyan, and S. N. Waterman (2014), Finescale parameterizations of turbulent dissipation, *J. Geophys. Res. Oceans*, *119*, 1383–1419, doi:10.1002/2013JC008979.
Saenko, O. A., X. Zhai, W. J. Merryfield, and W. G. Lee (2012), The combined effect of tidally and eddy-driven diapycnal mixing on the large-scale ocean circulation, *J. Phys. Oceanogr.*, *42*(4), 526–538.
Salehipour, H., and W. R. Peltier (2015), Diapycnal diffusivity, turbulent Prandtl number and mixing efficiency in Boussinesq stratified turbulence, *J. Fluid Mech.*, *775*, 464–500.
Salehipour, H., W. R. Peltier, and A. Mashayek (2015), Turbulent diapycnal mixing in stratified shear flows: The influence of Prandtl number on mixing efficiency and transition at high reynolds number, *J. Fluid Mech.*, *773*, 178–223.
Schumann, U., and T. Gerz (1995), Turbulent mixing in stably stratified shear flows, *J. Appl. Meteor.*, *34*(1), 33–48.
Shih, L. H., J. R. Koseff, G. N. Ivey, and J. H. Ferziger (2005), Parameterization of turbulent fluxes and scales using homogeneous sheared stably stratified turbulence simulations, *J. Fluid Mech.*, *525*, 193–214.
Smyth, W., and J. Moum (2013), Marginal instability and deep cycle turbulence in the eastern equatorial Pacific Ocean, *Geophys. Res. Lett.*, *40*(23), 6181–6185.
Smyth, W. D., J. Moum, and D. Caldwell (2001), The efficiency of mixing in turbulent patches: Inferences from direct simulations and microstructure observations, *J. Phys. Oceanogr.*, *31*, 1969–1992.

St. Laurent, L., A. C. Naveira Garabato, J. R. Ledwell, A. M. Thurnherr, J. M. Toole, and A. J. Watson (2012), Turbulence and diapycnal mixing in Drake Passage, *J. Phys. Oceanogr.*, *42*(12), 2143–2152.
Strang, E. J., and H. J. S. Fernando (2001), Entrainment and mixing in stratified shear flows, *J. Fluid Mech.*, *428*, 349–386.
Talley, L. D. (2013), Closure of the global overturning circulation through the Indian, Pacific, and Southern Oceans: Schematics and transports, *Oceanography*, *26*(1), 80–97.
van Haren, H., L. Gostiaux, E. Morozov, and R. Tarakanov (2014), Extremely long Kelvin-Helmholtz billow trains in the Romanche Fracture Zone, *Geophys. Res. Lett.*, *41*(23), 8445–8451.
Venayagamoorthy, S. K., and D. D. Stretch (2010), On the turbulent Prandtl number in homogeneous stably stratified turbulence, *J. Fluid Mech.*, *644*, 359–369.
Vettoretti, G., and W. R. Peltier (2015), Interhemispheric air temperature phase relationships in the nonlinear Dansgaard-Oeschger oscillation, *Geophys. Res. Lett.*, *42*(4), 1180–1189.
Walter, R., M. Squibb, C. Woodson, J. Koseff, and S. Monismith (2014), Stratified turbulence in the nearshore coastal ocean: Dynamics and evolution in the presence of internal bores, *J. Geophys. Res. Oceans*, *119*(12), 8709–8730.
Waterhouse, A. F., et al. (2014), Global patterns of diapycnal mixing from measurements of the turbulent dissipation rate, *44*, 1854–1872
Watson, A. J., J. R. Ledwell, M.-J. Messias, B. A. King, N. Mackay, M. P. Meredith, B. Mills, and A. C. N. Garabato (2013), Rapid cross-density ocean mixing at mid-depths in the Drake Passage measured by tracer release, *Nature*, *501*(7467), 408–411.
Whalen, C., L. Talley, and J. MacKinnon (2012), Spatial and temporal variability of global ocean mixing inferred from Argo profiles, *Geophys. Res. Let.*, *39*(18), L18612.
Whalen, C., J. MacKinnon, L. Talley, and A. Waterhouse (2015), Estimating the mean diapycnal mixing using a finescale strain parameterization, *J. Phys. Oceanogr.*, *45*, 1174–1188.
Winters, K. B., and E. A. D'Asaro (1996), Diascalar flux and the rate of fluid mixing, *J. Fluid Mech.*, *317*, 179–193.
Winters, K. B., P. N. Lombard, J. J. Riley, and E. A. D'Asaro (1995), Available potential energy and mixing in density-stratified fluids, *J. Fluid Mech.*, *289*, 115–128.
Wunsch, C., and R. Ferrari (2004), Vertical mixing, energy, and the general circulation of the oceans, *Annu. Rev. Fluid Mech.*, *36*, 281–314.